FIP-nha, a fungal immunomodulatory protein from *Nectria haematococca*, induces apoptosis and autophagy in human gastric cancer cells via blocking the EGFR-mediated STAT3/Akt signaling pathway

Shu-Ying Li, Li-Zhen Hou, Ya-Xin Gao, Na-Na Zhang, Bei Fan, Fengzhong Wang [*]

Institute of Food Science and Technology, Chinese Academy of Agricultural Sciences, Beijing, China

ABSTRACT

FIP-nha, a fungal immunomodulatory protein from *Nectria haematococca*, has been demonstrated a broad spectrum of antitumor activity and cell selectivity against human cancers in our previous study. However, the effect and mechanism of FIP-nha on gastric cancer remains unclear. In this study, we systematically observed the cytotoxicity, biological effect, regulatory mechanism and interaction target of FIP-nha on human gastric cancer cell lines, AGS and SGC7901. Our results demonstrated that FIP-nha inhibited the growth of AGS and SGC7901 cells in a dose-dependent manner and exerted proapoptotic effects on both cells as confirmed by flow cytometry, DAPI staining and western blot analysis. Additionally, the exposure of AGS and SGC7901 to FIP-nha induced autophagy as indicated by western blot analysis, GFP-LC3 and mCherry-GFP-LC3 transfection and acridine orange staining. Furthermore, we found that FIP-nha decreased the phosphorylation of EGFR, STAT3 and Akt and inhibited activation effect of ligand factor EGF to EGFR and its downstream signal molecule STAT3 and Akt. Finally, we proved that FIP-nha located on the surface of gastric cancer cells and bound directly to the transmembrane protein of EGFR by immunoprecipitation, cellular localization, molecular docking, microscale thermophoresis assay. The above findings indicated that FIP-nha inhibited the growth of gastric cancer and induced apoptosis and autophagy through competitively binding to EGFR with EGF to blocking the EGFR-mediated STAT3/Akt pathway. In summary, our study provided novel insights regarding the activity of FIP-nha against gastric cancer and contributed to the clinical application of FIP-nha as a potential chemotherapy drugs that targeted EGFR for human gastric cancer.

1. Introduction

Gastric cancer (GC) is a very common malignant tumor that is ranked the fourth leading reason of cancer death in the world (Wang et al., 2020; Siegel et al., 2019), and the second morbidity and mortality in China (Chen et al., 2016; Zhang et al., 2018). Due to no specific clinical symptoms during the early stages, GC patients are always diagnosed in the advanced and metastatic stages (Giuppi et al., 2021; Zeinali et al., 2020). Besides, the high aggression and heterogeneity of GC make its treatment very difficult (Abuderman, 2019). Chemotherapy has been indicated to be helpful in GC therapy. However, several reasons such as the cytotoxic effects and occurrence of drug resistance restrict the treatment of GC [6.8]. Therefore, it is urgent to prevent early, discover new drugs and explore new treatment methods. At present, it becomes

an important direction to find edible and medicinal materials and explore their functional factors in prevention and treatment of GC (Li et al., 2021).

Macrofungi, mainly represented by mushrooms, with a history of more than two thousand years as edible and medicinal resources (Wasser and Weis, 1999; Lindequist, 2013), have been believed to have health benefits including immunomodulatory, antitumour, antioxidant, antiviral, anti-microbial and hepatoprotective activities (Liu et al., 2015; Wong et al., 2009; Roupas et al., 2012). Up to now, a great deal of active compounds have been isolated from mushroom fruiting bodies, mycelium and spores (Wu et al., 2013). The extracts, such as polysaccharides (Li et al., 2015), polyphenols (Chen et al., 2008); terpenoids (Zhao et al., 2021); polysaccharide-peptide complex (Ho et al., 2004) and proteins (Jeurink et al., 2008) were reported to possess antitumor effects (Jiao

et al., 2020). In addition, a series of small active proteins known as fungal immunomodulatory proteins (FIPs) have been found in past decades, and showed significant effects against various cancers including human leukemia, liver cancer, lung cancer, and GC (Ejike et al., 2020).

FIPs have been classified as a new family due to their similar sequence and structure characteristics (Li et al., 2017). From 1989 until now; nearly 30 FIPs have been identified. Some of the FIPs have been identified by extracting or homologous cloning methods from macrofungi, others are identified by sequence similarity searching from the burgeoning genome databases (Ejike et al., 2020; Li et al., 2017). In addition to antitumor by activating the immune system; FIPs exhibit direct cytotoxicity to cancer cells. Moreover, FIPs also show direct cell toxicity against drug-resistant tumor cells (Li et al., 2014; Chiu et al., 2015). FIPs inhibit tumor growth through a variety of effects; such as apoptosis, autophagy, premature senescence, and cell cycle arrest (Carrola et al., 2011; WangXF et al., 2012). FIPs have been shown to exhibit several inhibitory effects on NSCLC and multidrug-resistant lung cancer cells. The mechanisms by which FIPs regulate lung cancer cells death have been intensively studied (Ejike et al., 2020).

FIP-nha is firstly identified in the ascomycete *Nectria haematococca* by using genome mining and represents a new FIP discovered beyond Basidiomycota (Bastiaan-Net et al., 2013). Previous studies have shown that FIP-nha exerts a variety of important biological activities (Li et al., 2014). Indeed, FIP-nha showed highly selective cytotoxicity in GC cells in our previous study (Li et al., 2014). However, the molecular mechanism by which FIP-nha inhibits GC cells remains unclear. In this study, combined with previous studies, using human GC cell lines AGS and SGC7901 as model cells, the recombinant expressed FIP-nha was systemically subjected to proliferation, apoptosis, autophagy, mechanism and target exploration to evaluate its antitumor effect.

2. Materials and methods

2.1. Expression and purification of FIP-nha

FIP-nha was expressed and purified as previously described (Li et al., 2014). The expression and purification of GFP-FIP-nha were detailed in the supplementary material S1.

2.2. Cell culture

The human GC cell lines AGS and SGC7901 and the normal gastric mucosa cell line GES-1 were obtained from American Type Culture Collection (ATCC; Manassas, VA, USA). The cells were cultured in Dulbecco's modified Eagle's medium (DMEM; high glucose; Gibco; Thermo Fisher Scientific, Inc., Waltham, MA, USA), supplemented with 10% fetal bovine serum (FBS; Life Technologies, Inc., Rockville, MD, USA), 100 μg/mL streptomycin, and 100 U/mL penicillin (Life Technologies, Inc., Rockville, MD, USA) at 37 °C in a humidified incubator containing 5% CO_2. Cells were passaged at 80–90% culture solution and were used for experiments in the exponential growth phase.

2.3. Cytotoxic assay

Cells were incubated in 96-well plates for 24 h, and then exposed to the indicated concentrations of FIP-nha (2.5, 5, 10, 20, 30, and 40 μg/mL) or GFP-FIP-nha (AGS: 4.5 μg/ mL, SGC7901:15 μg/ mL) for 24 h. The 10 mM PBS buffer (pH7.3) was used as negative control. Cell viabilities were evaluated with an MTT assay. The absorbance was measured at 490 nm by automated microplated reader (BioTek Instruments, Inc., Winooski, VT, USA). The cell death rate of FIP-nha on the cells was calculated as follows: inhibition rate (%) = (average A_{490} of the control group - average A_{490} of the experimental group)/(average A_{490} of the control group - average A_{490} of the blank group) × 100%. The IC_{50} value was determined as the concentration that caused 50% inhibition of cell proliferation.

2.4. Cell morphology observation

Cells were inoculated into 12-well plates for 24 h and then exposed to different concentrations of FIP-nha or GFP-FIP-nha for 24 h. Different fields of vision were selected under light microscope (IX70; Olympus Corporation, Tokyo, Japan) at 20x lens.

2.5. Cell viability assay

Cells were plated in 96-well plates and exposed to different concentrations of FIP-nha or negative control (PBS) for 0, 12, 24, and 48 h. Cell viability was examined with an MTS assay (Sigma, USA), 20 μL of MTS was added to each well and incubated for 1 h, after which the absorbance of the MTS signal was calculated after absorbance detection at 490 nm.

2.6. Colony formation assay

Cells were seeded evenly at 500 cells/well in six-well plates and treated with FIP-nha for 24 h. After the medium had been altered with fresh every 2 days for 14 days, plates were stained with 0.2% gentian violet and the colonies were counted under light microscope (IX70; Olympus Corporation, Tokyo, Japan).

3. 2.7. Apoptosis detection by flow cytometry

The cells were seeded into 6-well plates at 4×10^5 cells/well, cultured for 24 h, and treated with different concentrations of FIP-nha for 24 h. Apoptosis analysis was performed using an Annexin V-FITC Staining Kit (BD Biosciences, San Jose, CA, USA) following the manufacturer's instructions. All data were evaluated by BD Facscanto II flow cytometry (Becton Dickinson, San Jose, CA, USA).

3.1. Apoptosis detection by DAPI staining

Cells were seeded into 12-well plates with sterile glass sheets at 1×10^5 cells/well, cultured for 24 h, and treated with different concentrations of FIP-nha for 24 h. Then, the cells were fixed using 4 % paraformaldehyde for 15 min and permeabilized using 0.1 % Triton-X-100 for 10 min at RT. DAPI with a final concentration of 1:500 (in PBS) was utilized for staining. Depending on the morphological characteristics, the cells were recognized as normal or apoptotic. Cytation 5 cell imaging system (BioTeK, Winooski, VT, USA) was used to perform imaging.

3.2. Autophagosome detection

GC cells were transfected with pQCXIP-GFP-LC3 or pmCherry-GFP-LC3 plasmid using the Lipofectamine 3000 (Invitrogen; Thermo Fisher Scientific, Inc., Waltham, MA, USA) according to the recommended protocol by the manufacturer. After 6 h, the transfected cells were treated with different concentrations of FIP-nha for 24 h and then fixed in 4% paraformaldehyde for 20 min. The percentage of the cells with fluorescent dots was counted. For visualization of cell nucleus, DAPI staining was used. Sections were observed using an Olympus laser scanning confocal microscope with imaging software (Olympus Fluoview FV-1000, Tokyo, Japan).

3.3. Acridine orange staining

The cells were treated with FIP-nha for 24 h and then stained with 1 μg/mL acridine orange at 37 °C for 15 min. The formation of acidic ventricular septum was observed under fluorescence microscope.
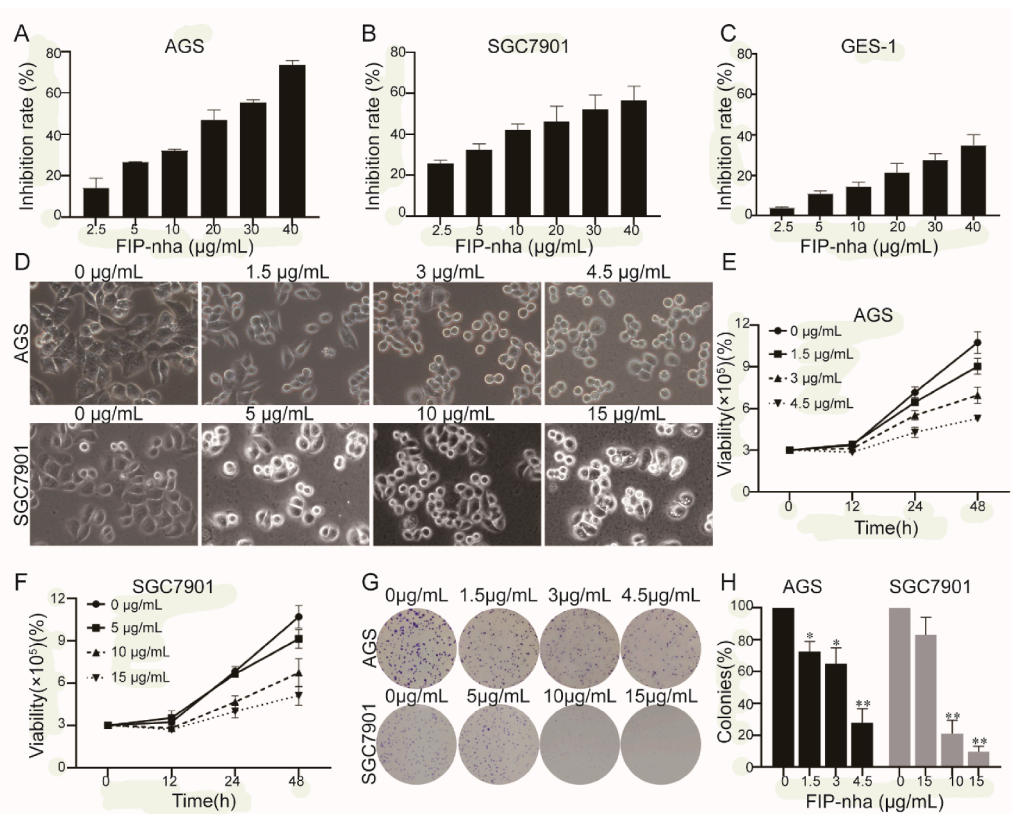
Fig. 1. FIP-nha inhibited growth of GC cells. (A-C): The inhibitory effects of FIP-nha on AGS, SGC7901, and GES-1 cells analyzed by MTT assay. (D): The morphology images of AGS and SGC7901cells treated with FIP-nha at the indicated concentrations. (E, F): The cell viabilities of AGS and SGC7901 cells analyzed by MTS assay. (G, H): The colony formation assays of AGS and SGC7901 cells treated with FIP-nha atthe indicated concentrations. *, $P < .05$; **, $P < .01$.

3.4. Immunoprecipitation

After cultured for 24 h, AGS and SGC7901 cells were instantaneously co-transfected with the expression vectors of Myc-EGFR and HA-Rubicon or HA-Rubicon and Flag-Beclin1. The transfected cells were cultured for 6 h, then the transfected cells were treated with different concentrations of FIP-nha (AGS: 4.5 µg/ml, SGC7901: 15 µg/ mL) for 24 h and lysed by RIPA lysate. Labeled antibodies and Protein G beads were added to the lysate, and western blot was used to detect the binding of Rubicon with EGFR or Beclin 1.

3.5. Western Blotting

After 20 min ice bath lysis with RIPA lysate (BioVision, San Francisco, USA), the supernatant protein lysate was taken and centrifuged at 12,000 RPM at 4 °C for 10 min. The protein concentration was determined by theBradford method. The corresponding volume of SDS was added to make the protein denatured at 99 °C for 5 min. After SDS-PAGE electrophoresis, PVDF membrane was transferred, sealed with 5% skim milk, primary antibody was incubated at 4 °C overnight, and secondary antibody labeled with horseradish peroxidase was incubated at room temperature for 2 h. ECL Western Blotting Detection Kit (GeneCopoeia, Rockville, MD, USA) was used for detection.Primary antibodies against PARP, pro-caspase-3, pro-caspase-8, LC3II, Beclin1, p62, pEGFR, EGFR, pSTAT3, STAT3, pAkt, Akt, Myc-EGFR, HA-Rubicon, Flag-Bedin1, HA-Rubicon, Flag-Rubicon and GAPDH and the secondary antibody (goat anti-rabbit antibody conjugated to horseradish peroxidase) were all purchased from Cell Signaling Technology, Inc. (Danvers, MA, USA).

3.6. Molecular docking

The structure of FIP-nha was modeled by Modeller 9.20 with the crystal structure of FIP-gmi (3KCW) as template. The structure of EGFR (PDB code: 3P0Y) was obtained from the protein data bank. Molecular docking studies were performed with Autodock 4. ZDOCK algorithm was used to simulate the docking between EGFR and FIP-nha. The lowest energy conformation was selected after docking for 100 times.

3.7. Microscale thermophoresis assay (MST)

EGFR was labeled with the Monolith™ Red-NHS SECOND-generation Protein Labeling Kit (MO-L011, NanoTemper Technologies GmbH, Munich, Germany). FIP-nha was diluted in different concentration gradients. Mixed the different concertation of FIP-nha with labelled EGFR and incubated for 30 min at room temperature. The specimens were loaded and measured on a Monolith NT.115 instrument (Nano Temper Technologies, München, Germany). The dissociation constant (Kd) and the signal-to-noise ratio (S/N) were fitted by the NT Analysis software (Nano Temper Technologies, München, Germany).

3.8. Statistical analysis

Statistical analysis was carried out with GraphPad Prism 7. Differences were analyzed using one-way ANOVA or a two-sample equal variance Student's *t*-test. Data are expressed as the mean ± SD. $P < .05$, $P < .01$ and $P < .001$were deemed to be statistically significant.
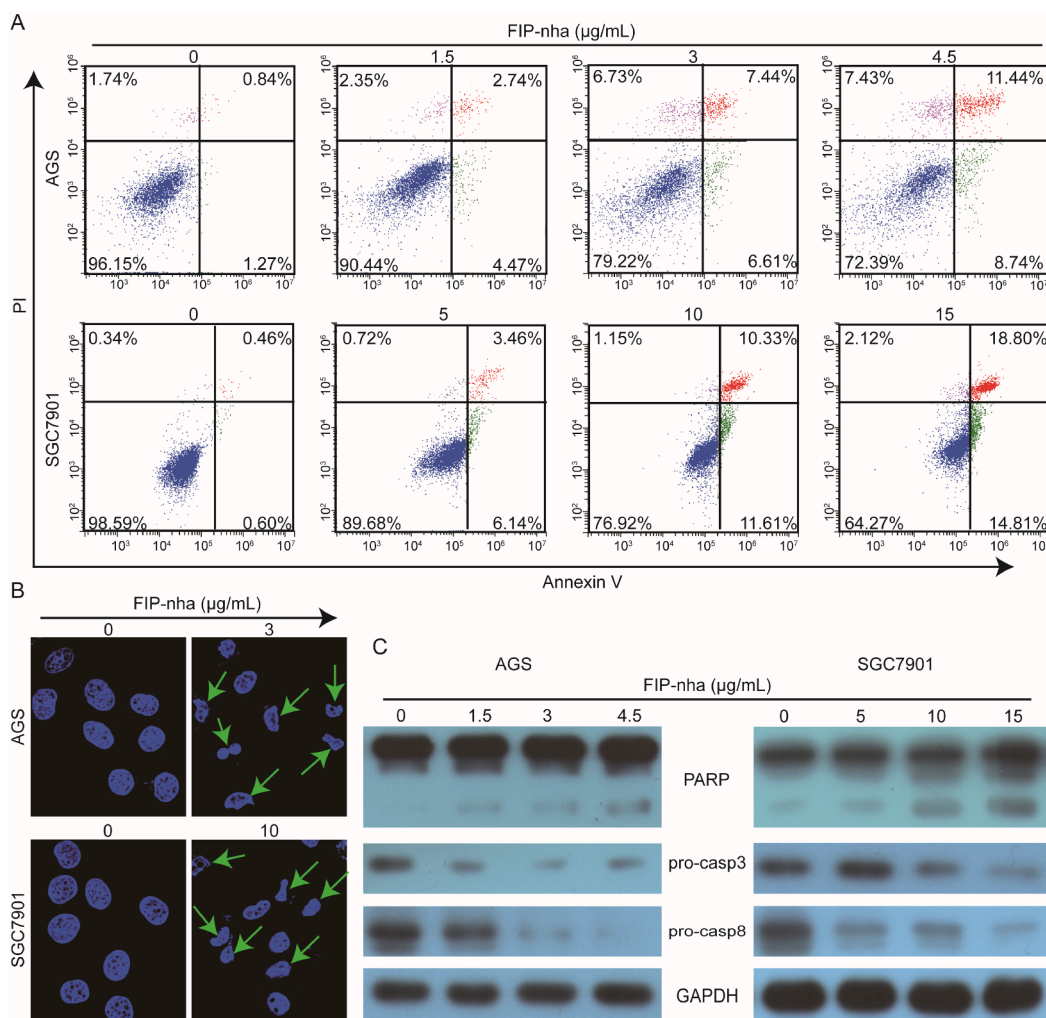
Fig. 2. FIP-nha induced apoptosis in GC cells. (A): AGS and SGC7901 cells were treated with increasing concentrations of FIP-nha for 24 h. Apoptotic induction was determined by flow cytometric analysis of Annexin V and PI-staining. The upper right quadrant (UR) represented late apoptotic cells stained with Annexin V and PI, and the lower right quadrant (LR) represented early apoptotic cells stained with Annexin V. (B): The nuclear morphology evaluation of AGS and SGC7901 cells, treated with the indicated concentration of FIP-nha, was detected by DAPI staining. (C): AGS and SGC7901 cells were treated with increasing concentrations of FIP-nha for 24 h. Western blot was performed using antibodies indicated. GAPDH was used as the loading control.

4. Results

4.1. FIP-nha inhibits the proliferation of GC cells

To explore the anti-GC activity of FIP-nha, we examined cell growth and proliferation in two GC cell lines, AGS and SGC7901. The cells were exposed to different concentrations of FIP-nha for the indicated durations, followed by analysis by MTT, MTS, and colony formation assays. MTT assays showed that viability in both AGS and SGC7901 was dose-dependently suppressed by FIP-nha (Fig. 1A and 1B). We also assessed whether FIP-nha was toxic to normal human gastric mucosal cells (GES-1), and the results showed that FIP-nha was weakly cytotoxic to normal gastric cells (Fig. 1C). The IC$_{50}$ of FIP-nha was 36.46 μg/mL, 37.08 μg/mL and 58.68 μg/mL in AGS, SGC7901 and GES-1 respectively. Subsequently, microscopy images showed obvious cellular shrinkage after FIP-nha treatment, with significantly decreased cellular attachment in comparison with controls (0 μg/mL) (Fig. 1D). Moreover, the results of MTS assays indicated that the cytotoxic effects of FIP-nha on these two GC cells line not only increased with increasing dose but also with exposure time (Fig. 1E and 1F). Furthermore, colony formation assays suggested that FIP-nha treatment markedly suppressed proliferation in AGS and SGC7901 cells compared to controls (Fig. 1G and 1H). These findings indicated that FIP-nha specifically inhibited the anchorage-dependent (cell proliferation) and anchorage-independent (colony formation) growth of GC cells.

4.2. FIP-nha induces apoptosis in GC cells

To confirm the apoptotic effects of FIP-nha on AGS and SGC7901 cells, we performed flow cytometry after Annexin V and PI staining and found that FIP-nha caused both early and late apoptosis in a dose-dependent manner. As shown in Fig. 2A, the percentage of apoptotic AGS cells was 2.11% in the control group (0 μg/mL) and reached 7.21%, 14.05%, and 20.18% in the treatment groups with 1.5, 3 and 4.5 μg/mL, respectively; for SGC7901 cells, the percentage of apoptotic cells was 1.06% in the control group and 9.60%, 21.94%, and 33.61% in the treatment groups with 5, 10 and 15 μg/mL, respectively. These results prove that the percentage of apoptotic cells increased markedly with increasing doses of FIP-nha. The above results indicated that FIP-nha could induce apoptosis in GC cells. DAPI staining was used ulteriorly to evaluate changes in nuclear morphology of apoptotic AGS and SGC7901 cells. After FIP-nha treatment, cell nuclear shrinkage, which are typical apoptotic morphological characteristics, were significantly increased in the two GC cell lines compared to the controls (Fig. 2B). The cleavage expressions of apoptosis-related proteins caspase-3, caspase-8 and PARP were detected by western blot. The results showed that with the increased dose of FIP-nha, the enzyme precursor of caspase-3 (pro-caspase-3) and caspase-8 (pro-caspase-8) were significantly down-regulated, and the expression of PARP cleavage bands showed an obvious trend of increase (Fig. 2C). These results suggested that FIP-nha induced caspase-mediated apoptosis in GC cells.
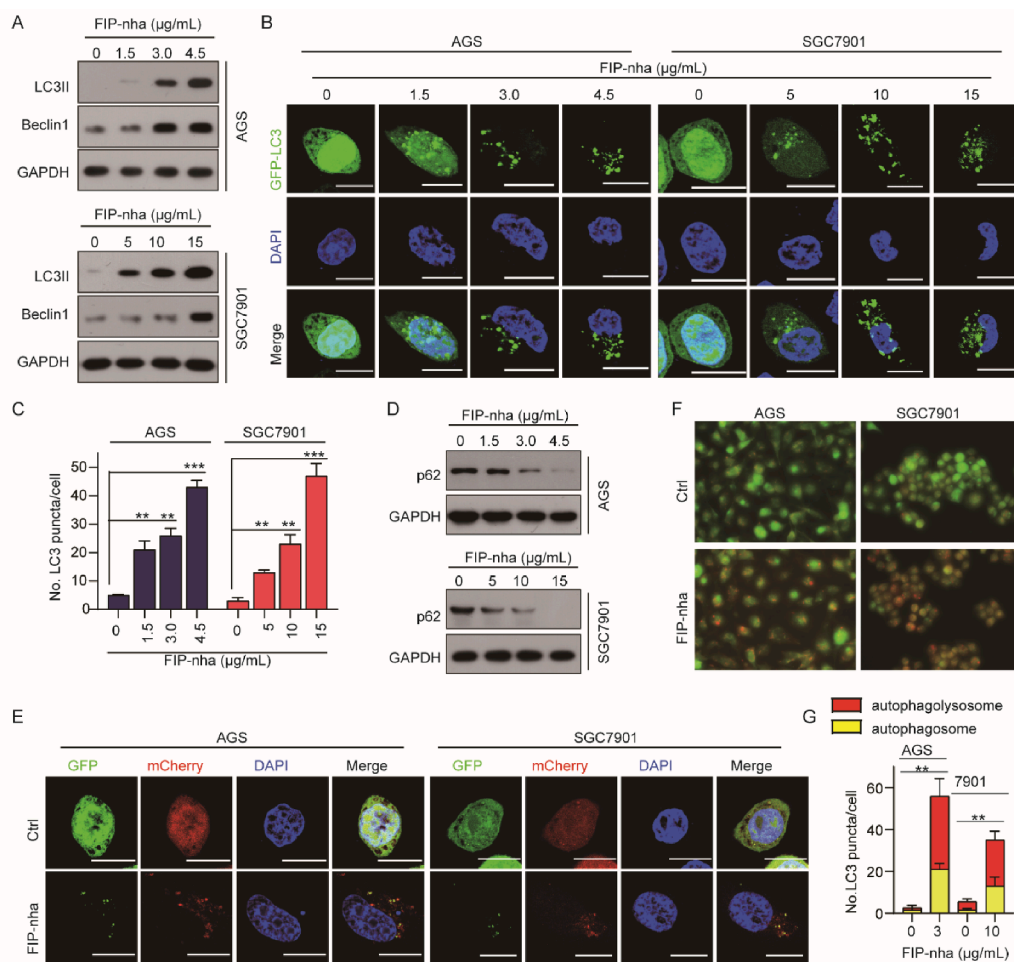
Fig. 3. FIP-nha induced autophagy in GC cells. (A, D): AGS and SGC7901 cells were treated with increasing concentrations of FIP-nha for 24 h. Western blot was performed using antibodies indicated. GAPDH was used as the loading control. (B): AGS and SGC7901 cells transfected with pQCXIP-GFP-LC3 plasmid were treated with increasing concentrations of FIP-nha for 24 h, and assessed by immunofluorescence analyses. Scale bar = 20 μm. (C): Graph shows quantification of LC3-positive punctate cells in (B). (E-F): AGS and SGC7901 cells transfected with pQCXIP-GFP-LC3 or pmCherry-GFP-LC3 plasmids were treated with indicated concentration of FIP-nha for 24 h, and assessed by immunofluorescence analyses. (G): Graph shows quantification of LC3-positive punctuate cells in (F). Scale bar = 20 μm. **, $P < .01$; ***, $P < .001$.

4.3. FIP-nha induces autophagy in GC cells

To test whether FIP-nha could induce autophagy in GC cells, the expression of autophagy-related proteins LC3II and Beclin 1 were detected by western blot. The results showed that FIP-nha induced the accumulation of LC3II and Beclin1 in AGS and SGC7901 cells in a dose-dependent fashion(Fig. 3A), suggesting that FIP-nha may induce autophagy in GC cells. Accordingly,the pQCXIP-GFP-LC3 plasmid was transfected into AGS and SGC7901 cells which were then treated with FIP-nha for 24 h, followed by confocal microscopy assessment to detect the formation of autophagosomes. The results showed that while control cells displayed diffuse staining, AGS and SGC7901 cells upon FIP-nha treatment exhibited a speckled fluorescent staining pattern, indicating the formation of autophagosomes and the redistribution of LC3 to autophagosomes (Fig. 3B, C). The accumulation of autophagosomes is caused by increased autophagosome formation or hindered lysosomal degradation (i.e. blocked autophagy flux). The expression of p62 can reflect the change of autophagy flux. Western blot investigation of p62 expression level showed that p62 was significantly decreased in both GC cell lines after FIP-nhatreatment (Fig. 3D), indicating autophagy flux was unblocked. Furthermore, autophagy flux was detected by double fluorescent plasmid, mCherry-GFP-LC3, transfection. Yellow and red fluorescence were significantly increased (Fig. 3E), indicating fusion of autophagosomes and lysosomes, i.e., FIP-nha promoted autophagy flux. Acridine orange staining was used to detect the lysosomal activity of the two GC cell lines. It was found that the red fluorescence was significantly enhanced after FIP-nha treatment (Fig. 3F, G), indicating that FIP-nha reduced the pH value of the acid compartment and promoted the

lysosomal activity. In conclusion, the above experiments showed that FIP-nha activated autophagy in GC cells and promoted autophagy flux.

4.4. FIP-nha inhibits the proliferation of GC cellsviablocking EGFR/STAT3/Akt signaling

Epidermal growth factor receptor (EGFR), a transmembrane glycoprotein, is one of the four members of the ErbB family of tyrosine kinase receptors. Dimerization activation leads to phosphorylation of autotyrosine kinases, which in turn activates STAT3 and Akt, the downstream signaling proteins of EGFR, promoting cell proliferation, survival and metastasis (Huang et al., 2019). Western blot analysis showed that FIP-nha down-regulated the phosphorylation of EGFR (Y1068) in both cell lines, but had no significant effect on total EGFR protein (Fig. 4A). The expression and activation of EGFR downstream signaling molecules were further investigated. It was found that phosphorylation levels of STAT3 and Akt were down-regulated with increasing FIP-nha dose, while total protein did not change significantly (Fig. 4B). Continuous activation of STAT3 and Akt promotes the malignant progression of various tumor cells. As can be seen from the above results that FIP-nha may inhibit GC cell proliferationby inhibiting STAT3 and Akt activities mediated by blocking EGFR activation. The epidermal growth factor (EGF) is a ligand factor of EGFR and plays an important role in the sustained activation of EGFR in a variety of cancers. Further test whether FIP-nha can overcome the growth-promoting effect of EGF on GC cells. MTT assay found that FIP-nha significantly inhibited the promoting effect of EGF on GC cell proliferation (Fig. 4C-D). The antagonistic effect of FIP-nha on EGF activation of EGFR and its downstream signal was
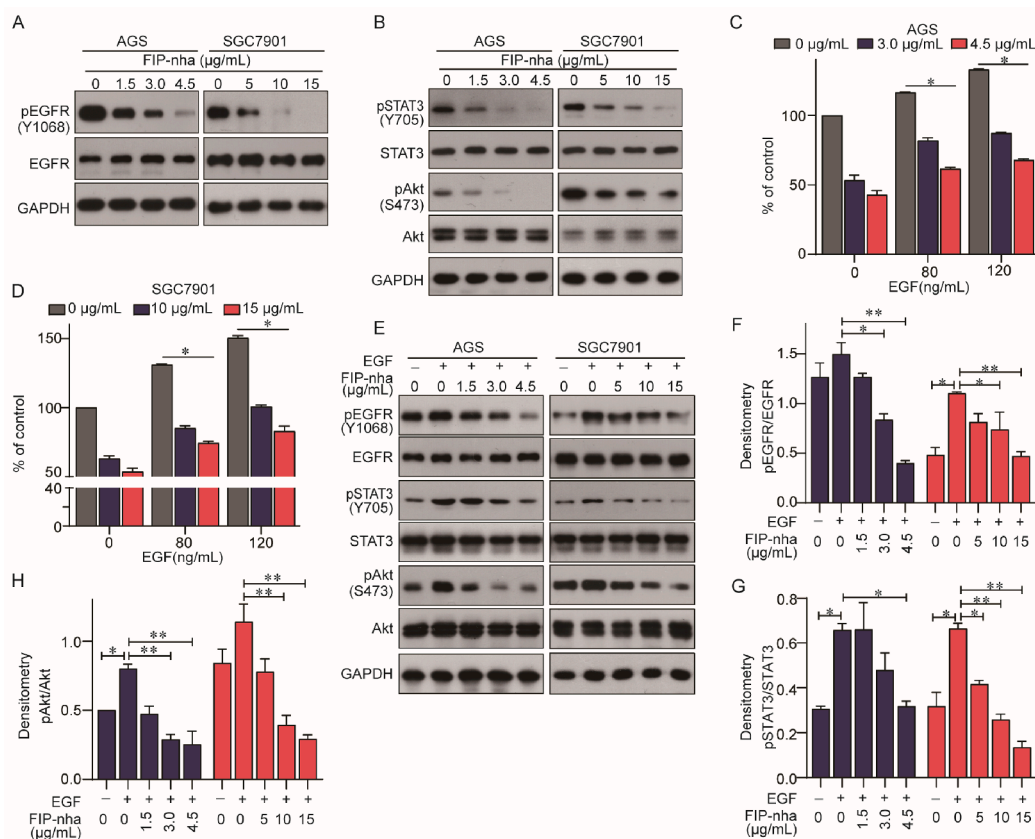
Fig. 4. FIP-nha inhibited proliferation of GC cells through inactivating the EGFR/STAT3/Akt signaling. (A, B): AGS and SGC7901 cells were treated with increasing concentrations of FIP-nha for 24 h. Western blot assay was performed using antibodies indicated. (C, D): AGS and SGC7901 cells were treated with increasing concentrations of FIP-nha and EGF for 24 h. MTT assay was performed. (E): AGS and SGC7901 cells were treated with 120 ng/mL EGF and different concentrations of FIP-nha for 24 h. Western blot assay was performed using antibodies indicated.(F-H): Graph shows quantification of pEGFR/EGFR, pSTAT3/STAT3 and pAkt/Akt in (E). *, $P < .05$; **, $P < .01$.

further detected. Western blot results showed that EGF significantly activated EGFR and its downstream STAT3 and Akt, while FIP-nha treatment significantly inhibited EGF's activation of EGFR and its downstream STAT3 and Akt (Fig. 4E-H). These results indicated that FIP-nha inhibited the activity of EGFR and its downstream signal molecules by antagonizing the activation of EGF.

4.5. FIP-nha blocks EGFR/STAT3/Akt pathwayby directly binding to EGFR

Previous studies have reported that kinase inactivation of EGFR interacts with Rubicon, a Beclin1-binding autophagy inhibitor. Binding of inactive EGFR to Rubicon can promote the dissociation of Rubicon and Beclin1, thus activating autophagy (Sooro et al., 2018). The binding of Rubicon with EGFR orBeclin1 before and after FIP-nha treatment was detected by immunoprecipitation. The results showed that FIP-nha enhanced the binding of Rubicon to EGFR, but reduced the binding of Rubicon to Beclin1 (Fig. 5A-B). To clarify the localization of FIP-nha in GC cells, GFP-FIP-nha vector was constructed and GFP-FIP-nha protein was purified. After GC cells was treated with GFP-FIP-nha, the localization of GFP-FIP-nha was observed under a microscope, and it was found that GFP-FIP-nha was mainly located on the surface of GC cells (Fig. 5C). The 3D structure of FIP-nha was constructed by homology modeling, and the quality of the model was evaluated by PROCHECK (Fig. 5D). Ramachandran diagram was generated, where the allowable area and additional allowable area were 87.5% and 11.5%, respectively, and amino acid residues accounted for 99% within the reasonable range (Fig. 5E). In view of the effect of FIP-nha on EGFR, we simulated the binding of FIP-nha to the extracellular segment of EGFR by molecular docking (Fig. 5F-H). The results showed that FIP-nha protein interacted with the extracellular segment of EGFR. Residues of Pro349, Arg353, Ser356, Phe357, His359 and Pro362 on the chain of EGFR interact with sites of Asn6, Val10, Tyr13, Gln97, Tyr99, Gln108, Tyr109 and Leu110

on FIP-nha. The main forces are hydrophobic interaction, van der Waals force, hydrogen bond and electrostatic force. His359 of EGFR formeda hydrogen bond with Gln97 of FIP-nha with a bond length of 3.24 Å. The Ser356 residueof EGFR and Leu110 of FIP-nha formed two hydrogen bonds with bond lengths of 2.78 Å and 2.78 Å respectively. The formation of these hydrogen bonds enhanced the binding force of the two proteins, which may inhibit the binding of EGFR to its ligand EGF and in turn affected the activation of the downstream signaling molecules of EGFR.In order to further clarify the direct binding effect of FIP-nhawith EGFR, we tested the binding effect of FIP-nhawith EGFR by MST (Fig. 5I). The results showed that FIP-nha had a strong binding effect with EGFR. The dissociation constant (Kd) was 15.54 ± 2.93 μmol/L, and the signal-to-noise ratio (S/N) was 19.5. The above values indicated that there was a strong direct binding between FIP-nha and EGFR.

5. Discussion

This is the first report of systematical study the toxicity, effects, mechanisms and interaction targets of FIP-nha on GC cell lines, AGS and SGC7901. This study proved that FIP-nha had stronger antitumor activity and cell selectivity on two types of GC cell lines in a dose-dependence manner. Further exploration of the antitumor effect and mechanism confirmed that FIP-nha induced apoptosis and autophagy through blocking the EGFR/STAT3/Akt signal pathway. Finally, the interaction target studies confirmed that FIP-nha blocked the above signaling pathway by competitively binding EGFR with EGF. Therefore, FIP-nha can be further developed as an EGFR-targeting agent for the prevention and treatment of GC.

In addition to antitumor by activating the immune system, FIPs exhibit direct cytotoxicity to cancer cells. Moreover, FIPs also show direct cell toxicity against drug-resistant tumor cells (Li et al., 2014; Chiu et al., 2015). Previous studies have confirmed that some FIPs, such as FIPs from *Ganoderma* spp., show significant direct anti-tumor activity,
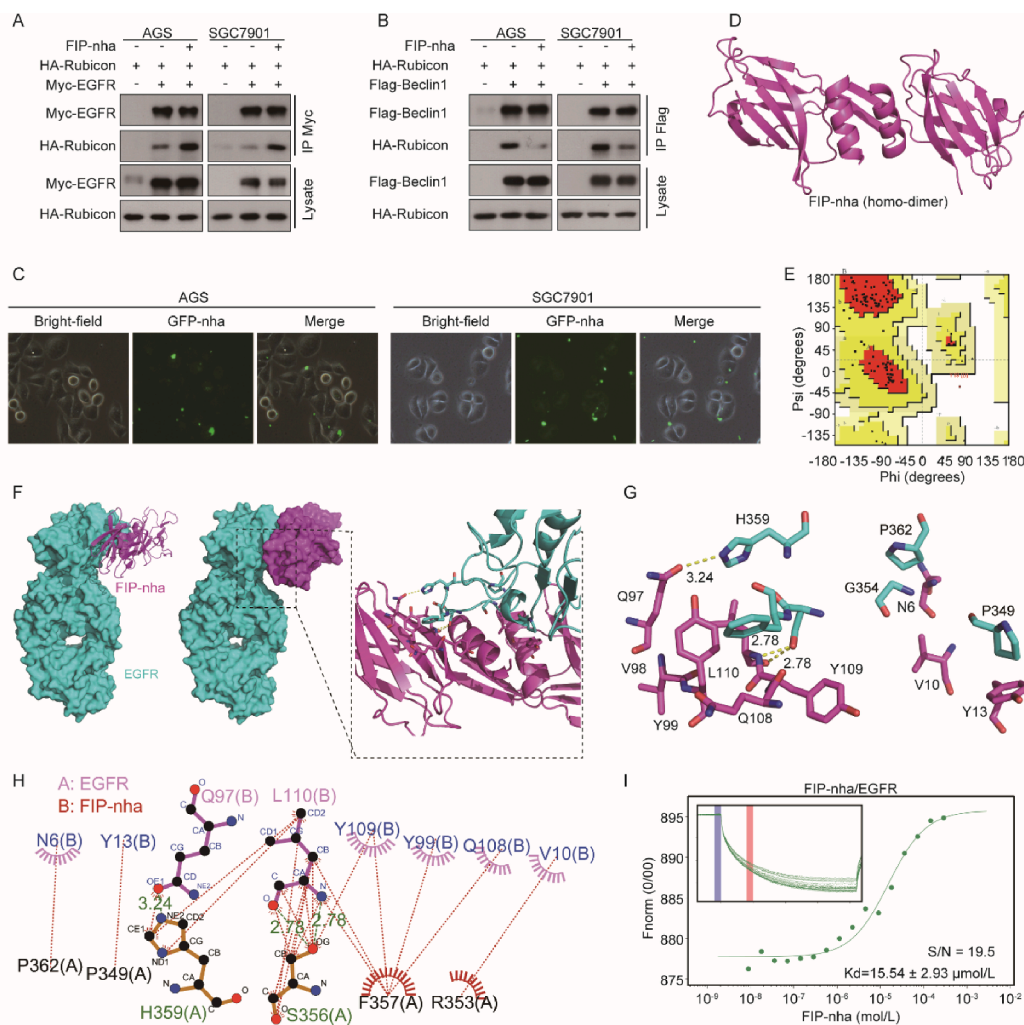
Fig. 5. FIP-nha activated autophagy in GC cells by directly binding to EGFR. (A,B): The effects of FIP-nha on the binding of EGFR to Rubicon or Rubicon to Beclin 1 were detected by immunoprecipitation. After cultured for 24 h, AGS and SGC7901 cells were treated with FIP-nha (AGS: 4.5 µg/mL, SGC 7901:15 µg/mL) for 24 h, respectively. Western blot assay was performed using antibodies indicated.(C): The localization analysis of FIP-nha. After cultured for 24 h, AGS and SGC7901 cells were treated with GFP-FIP-nha (AGS: 4.5 µg/mL, SGC 7901:15 µg/mL) for 24 h, respectively. The localization of GFP-FIP-nha was observed under fluorescence microscope, and the cell morphological changes were observed under microscopeat 20x lens. (D): FIP-nha structure was modeled by Modeller 9.20 software. FIP-nha mainly exists in the form of homodimer. Each monomer consists of an FNIII-like domain with an N-terminal a-helix and b-strand. (E): Analysis of pull conformation diagram. The proportion of amino acid residues in a reasonable range was more than 99% by Procheck Server evaluation.(F): The binding mode of FIP-nha docked into EGFR. EGFR is blue, FIP-nha is purple. (G, H) The interaction residues of FIP-nha with EGFR. (I): Binding affinity of FIP-nha with EGFR by MST in standard treated capillaries. (For interpretation of the references to colour in this figure legend, the reader is referred to the web version of this article.)

while some other FIPs, such as FIP-fve from *Flammulina velutipes*, show extremely weak direct anti-tumor activity. Comparative structural analysis indicated that the difference in the biological activity of these FIPs was due to significant local conformational changes at the Loop DE and Loop FG of the fibronectin type III (FNIII) domain, which may be a potential active region (Paaventhan et al., 2003; Huang et al., 2009).Our previous studies confirmed that FIP-nha highly overlapped in the above two loop regions with FIPs from *Ganoderma* spp. and showed significant and broad-spectrum anti-tumor activities (Li et al., 2014). In this study, we further confirmed that FIP-nha was significantly toxic to GC cells but had weak cytotoxicity on normal GES-1 cells.

FIPs inhibit tumor growth through a variety of effects, such as apoptosis, cell cycle arrest, premature senescence and autophagy (Carrola et al., 2011; WangXF et al., 2012). The anti-tumor effects of FIPs from different sources vary greatly. Such as FIPs from *Ganoderma* spp. shared considerably higher sequence and structural similarity, but their anti-tumor effects are variable. Thus far, four FIPs from *Ganoderma* spp., LZ-8 (*G. lucidum*), FIP-gts (*G. tsugae*), FIP-gmi (*G. microsporum*) and FIP-gsi (*G. sinensis*) have already been confirmed exhibited strong direct anti-tumor activity. LZ-8 has been shown to inhibit the proliferation of human glioblastoma and chronic myeloid granulocyte leukemia cells by inducing apoptosis (Cong et al., 2014). FIP-gts inhibits NSCLC cells growth, leading to G1 arrest, consequently inducing premature senescence (Liao et al., 2008). FIP-gts induces autophagic cell death against drug-resistant urothelial cancer cells (Li et al., 2014). FIP-gmi inhibits tumor growth and significantly induces autophagy, but not apoptosis, in

NSCLC and multidrug-resistant lung cancer cells (Chiu et al., 2015; Hsin et al., 2011). In this study, we proofed that FIP-nha suppressed GC cells proliferation by inducing apoptosis and autophagy.

However, clear evidence of the mechanisms by which FIPs regulate cancer cells death remains scarce. Using the NSCLC cells, A549, as the cell model, several researches have been performed to explore the anti-tumor mechanisms of FIPs. FIP-gts exhibits anti-tumor activity by regulating telomerase expression (Liao et al., 2006) and inhibits telomerase activity through nuclear export mechanisms and ER stress-induced intracellular calcium levels (Liao et al., 2007). FIP-gmi induces autophagy through the Akt-mTOR-p70S6K pathway, thereby inhibiting multidrug-resistant lung cancer cells (Chiu et al., 2015). FIP-fve suppresses lung cancer cell proliferation via p53 activation (Chang et al., 2013). In early studies, we confirmed that FIP-nha induced A549 cell apoptosis by activating p53, which then negatively regulating the PI3K-Akt-mTOR and/or AMPK pathway and causing subsequent metabolic disturbance of A549 cells (Xie et al., 2018; Wang et al., 2019). In this study, for the first time we deeply explored the mechanism of FIP-nha on GC cells and confirmed that FIP-nha inhibited GC cell proliferation by blocking the EGFR/STAT3/Akt signaling pathway.

Although recent advances in cancer biology have led to the identification of new targets and the development of novel-targeted therapies, the localization and interaction targets of FIPs in tumor cells still are a research blank. Elucidating the localization and determining the interaction partners of FIP-nha in inhibiting cancer metabolism will provide novel insights for anticancer research and offer promising therapeutic

targets for FIP-nha in cancer therapies.Our studies confirmed that FIP-nha located on the cell surface, competitively bound with EGF to the extracellular portion of the transmembrane protein EGFR, influenced its activation of downstream STAT3/Akt signaling pathways and ultimately prevented GC cells proliferation. EGFR is one of the key cancer-driving proteins and an important target of several anti-cancer therapies (Troiani et al., 2016). Activation of EGFR by its ligands such as EGF results in the receptor dimerization and; subsequently, autophosphorylation of a series of tyrosines in the C-terminal tail of the receptor which can influence different cellular effects including promotion of cell proliferation, protection against apoptosis, acceleration of invasion, and angiogenesis (Huang et al., 2019). After activation by EGF; the dimerization of EGFR allows the cross-phosphorylation of several tyrosine residues, including Y1068, the main binding site for STAT3 (Ta et al., 2018). Our data showed that the presence of FIP-nha significantly inhibited autophosphorylation of EGFR at Y1068; possibly by hindering EGFR dimerization, and thus the decreased EGFR association with STAT3.

Generally, the FIP-nha accumulates in the cell surface disturbed activation EGFR with EGF and inhibited the phosphorylation of EGFR, STAT3 and Akt, the activation of STAT3-mediated Akt pathway, and proliferation of GC cells.The effects of FIP-nha on GC cells provided a better understanding regarding the roles of FIP-nha in GC therapy and indicated its potential as a candidate for treating cancer in EGF-dependent EGFR activation.

6. Authors' contributions

Concept and design: F.Z.W. Experiments and procedures: S.Y.L., L.Z.H., and Y.X.G. Data analysis: S.Y.L. and N.N.Z. Writing and editing the article: S.Y.L. and B.F. All authors read and approved the final manuscript. All authors have made a sufficient contribution to the work.

Declaration of Competing Interest

The authors declare that they have no known competing financial interests or personal relationships that could have appeared to influence the work reported in this paper.

References

Wang, M., Zhao, H., Hu, J., Xu, Z., Lin, Y., Zhou, S., & Penicilazaphilone, C. (2020). a New Azaphilone, Induces Apoptosis in Gastric Cancer by Blocking the Notch Signaling Pathway. *Frontiers in Oncology, 10*, 116. https://doi.org/10.3389/fonc.2020.00116. PMID: 32117763; PMCID: PMC7026506

Siegel, R. L., Miller, K. D., & Jemal, A. (2019). Cancer statistics, 2019. *CA: A Cancer Journal for Clinicians, 69*(1), 7–34. https://doi.org/10.3322/caac.21551. Epub 2019 Jan 8. PMID: 30620402.

Chen, W., Zheng, R., Baade, P. D., Zhang, S., Zeng, H., Bray, F., Jemal, A., Yu, X. Q., & He, J. (2016). Cancer statistics in China, 2015. *CA: A Cancer Journal for Clinicians, 66*(2), 115–132. https://doi.org/10.3322/caac.21338. Epub 2016 Jan 25. PMID: 26808342.

Zhang, G., Li, J., Li, S., & Wang, Y. (2018). Exploring Spatial Trends and Influencing Factors for Gastric Cancer Based on Bayesian Statistics: A Case Study of Shanxi, China. *International Journal of Environmental Research and Public Health, 15*(9), 1824. https://doi.org/10.3390/ijerph15091824. PMID: 30142954; PMCID: PMC6165541

Giuppi, M., La Salvia, A., Evangelista, J., & Ghidini, M. (2021). The Role and Expression of Angiogenesis-Related miRNAs in Gastric Cancer. *Biology (Basel)., 10*(2), 146. https://doi.org/10.3390/biology10020146. PMID: 33673057; PMCID: PMC7918665

Zeinali, T., Karimi, L., Hosseinahli, N., Shanehbandi, D., Mansoori, B., Mohammadi, A., … Baradaran, B. (2020). Overexpression of miRNA-145 induces apoptosis and prevents proliferation and migration of MKN-45 gastric cancer cells. *EXCLI J., 19*,

1446–1458. https://doi.org/10.17179/excli2020-2777. PMID: 33250681; PMCID: PMC7689247

Abuderman, A. A. (2019). Gastric cancer & prospects of cancer in Saudi Arabia peninsula. *Saudi Journal of Biological Sciences., 26*(6), 1095–1100. https://doi.org/10.1016/j.sjbs.2018.02.016. Epub 2018 Feb 27. PMID: 31516334; PMCID: PMC6734134.

Li, S., Gao, J., Hou, L., Gao, Y., Sun, J., Zhang, N., … Wang, F. (2021). The Small Molecule Fractions of *Floccularialuteovirens* Induce Apoptosis of NSCLC Cells through Activating Caspase-3 Activity. *International Journal of Molecular Sciences, 22*(19), 10609. https://doi.org/10.3390/ijms221910609. PMID: 34638946; PMCID: PMC8508712

Wasser, S. P., & Weis, A. L. (1999). Therapeutic effects of substances occurring in higher Basidiomycetes mushrooms: A modern perspective. *Critical Reviews in Immunology, 19*(1), 65–96. PMID: 9987601.

Lindequist, U. (2013). The merit of medicinal mushrooms from a pharmaceutical point of view. *Int J Med Mushrooms., 15*(6), 517–523. https://doi.org/10.1615/intjmedmushr.v15.i6.10. PMID: 24266376.

Liu, X., Wang, L., Zhang, C., Wang, H., Zhang, X., & Li, Y. (2015). Structure characterization and antitumor activity of a polysaccharide from the alkaline extract of king oyster mushroom. *CarbohydrPolym., 118*, 101–106. https://doi.org/10.1016/j.carbpol.2014.10.058. Epub 2014 Oct 30 PMID: 25542113.

Wong, J. H., Wang, H., & Ng, T. B. (2009). A haemagglutinin from the medicinal fungus *Cordycepsmilitaris. Bioscience Reports, 29*(5), 321–327. https://doi.org/10.1042/BSR20080153. PMID: 19093913.

Roupas, P., Keogh, J., Noakes, M., Taylor, P., & Margetts, C. (2012). The role of edible mushrooms in health: Evaluation of the evidence. *Journal of Functional Foods, 4*(4), 687–709.

Wu, G. S., Guo, J. J., Bao, J. L., Li, X. W., Chen, X. P., Lu, J. J., & Wang, Y. T. (2013). Anti-cancer properties of triterpenoids isolated from *Ganoderma lucidum*-a review. *Expert OpinInvestig Drugs., 22*(8), 981–1922. https://doi.org/10.1517/13543784.2013.805202. Epub 2013 Jun 24 PMID: 23790022.

Li, S. C., Yang, X. M., Ma, H. L., Yan, J. K., & Guo, D. Z. (2015). Purification, characterization and antitumor activity of polysaccharides extracted from *Phellinus igniarius* mycelia. *CarbohydrPolym., 133*, 24–30. https://doi.org/10.1016/j.carbpol.2015.07.013. Epub 2015 Jul 13 PMID: 26344250.

Chen, W., Zhao, Z., Li, L., Wu, B., Chen, S. F., Zhou, H., … Li, Y. Q. (2008). Hispolon induces apoptosis in human gastric cancer cells through a ROS-mediated mitochondrial pathway. *Free RadicBiol Med., 45*(1), 60–72. https://doi.org/10.1016/j.freeradbiomed.2008.03.013. Epub 2008 Mar 29 PMID: 18423410.

Zhao, M., Tang, Y., Xie, J., Zhao, Z., & Cui, H. (2021). Meroterpenoids produced by fungi: Occurrence, structural diversity, biological activities, and their molecular targets. *European Journal of Medical Chemistry, 209*, Article 112860. https://doi.org/10.1016/j.ejmech.2020.112860. Epub 2020 Sep 28 PMID: 33032085.

Ho, J. C., Konerding, M. A., Gaumann, A., Groth, M., & Liu, W. K. (2004). Fungal polysaccharopeptide inhibits tumor angiogenesis and tumor growth in mice. *Life Sciences, 75*(11), 1343–1356. https://doi.org/10.1016/j.lfs.2004.02.021. PMID: 15234192.

Jeurink, P. V., Noguera, C. L., Savelkoul, H. F., & Wichers, H. J. (2008). Immunomodulatory capacity of fungal proteins on the cytokine production of human peripheral blood mononuclear cells. *IntImmunopharmacol., 8*(8), 1124–1133. https://doi.org/10.1016/j.intimp.2008.04.004. Epub 2008 May 7 PMID: 18550017.

Jiao, C., Chen, W., Tan, X., Liang, H., Li, J., Yun, H., … Yang, B. B. (2020). *Ganoderma lucidum* spore oil induces apoptosis of breast cancer cells in vitro and in vivo by activating caspase-3 and caspase-9. *Journal of Ethnopharmacology, 247*, Article 112256. https://doi.org/10.1016/j.jep.2019.112256. Epub 2019 Oct 3 PMID: 31586690.

Ejike, U. C., Chan, C. J., Okechukwu, P. N., & Lim, R. L. H. (2020). New advances and potentials of fungal immunomodulatory proteins for therapeutic purposes. *Critical Reviews in Biotechnology, 40*(8), 1172–1190. https://doi.org/10.1080/07388551.2020.1808581. Epub 2020 Aug 28 PMID: 32854547.

Li, S., Jiang, Z., Xu, W., Xie, Y., Zhao, L., Tang, X., … Xin, F. (2017). FIP-sch2, a new fungal immunomodulatory protein from *Stachybotryschlorohalonata*, suppresses proliferation and migration in lung cancer cells. *ApplMicrobiolBiotechnol., 101*(8), 3227–3235. https://doi.org/10.1007/s00253-016-8030-6. Epub 2017 Jan 12 PMID: 28078399.

Li, J. R., Cheng, C. L., Yang, W. J., Yang, C. R., Ou, Y. C., Wu, M. J., & Ko, J. L. (2014). FIP-gts potentiate autophagic cell death against cisplatin-resistant urothelial cancer cells. *Anticancer Research, 34*(6), 2973–2983. PMID: 24922662.

Chiu, L. Y., Hu, M. E., Yang, T. Y., Hsin, I. L., Ko, J. L., Tsai, K. J., & Sheu, G. T. (2015). Immunomodulatory Protein from *Ganoderma microsporum* Induces Pro-Death Autophagy through Akt-mTOR-p70S6K Pathway Inhibition in Multidrug Resistant Lung Cancer Cells. *PLoS ONE, 10*(5), Article e0125774. https://doi.org/10.1371/journal.pone.0125774. PMID: 25946033; PMCID: PMC4422711

Carrola, J., Rocha, C. M., Barros, A. S., Gil, A. M., Goodfellow, B. J., Carreira, I. M., … Duarte, I. F. (2011). Metabolic signatures of lung cancer in biofluids: NMR-based metabonomics of urine. *Journal of Proteome Research, 10*(1), 221–230. https://doi.org/10.1021/pr100899x. Epub 2010 Nov 23 PMID: 21058631.

Wang, X. F., Su, K. Q., Bao, T. W., Cong, W. R., Chen, Y. F., Li, Q. Z., & Zhou, X. W. (2012). Immunomodulatory Effects of Fungal Proteins. *Curr Top Nutraceuticals Res., 10*, 1–11.

Bastiaan-Net, S., Chanput, W., Hertz, A., Zwittink, R. D., Mes, J. J., & Wichers, H. J. (2013). Biochemical and functional characterization of recombinant fungal immunomodulatory proteins (rFIPs). *IntImmunopharmacol., 15*(1), 167–175. https://doi.org/10.1016/j.intimp.2012.11.003. Epub 2012 Nov 19 PMID: 23174509.

Li, S., Nie, Y., Ding, Y., Shi, L., & Tang, X. (2014). Recombinant expression of a novel fungal immunomodulatory protein with human tumor cell antiproliferative activity

from *Nectria haematococca. International Journal of Molecular Sciences, 15*(10), 17751–17764. https://doi.org/10.3390/ijms151017751. PMID: 25272229; PMCID: PMC4227187

Huang, Q., Li, S., Zhang, L., Qiao, X., Zhang, Y., Zhao, X., … Li, Z. (2019). CAPE-pNO2 Inhibited the Growth and Metastasis of Triple-Negative Breast Cancer via the EGFR/STAT3/Akt/E-Cadherin Signaling Pathway. *Frontiers in Oncology, 9*, 461. https://doi.org/10.3389/fonc.2019.00461. PMID: 31214503; PMCID: PMC6558049

Sooro, M. A., Zhang, N., & Zhang, P. (2018). Targeting EGFR-mediated autophagy as a potential strategy for cancer therapy. *International Journal of Cancer, 143*(9), 2116–2125. https://doi.org/10.1002/ijc.31398. Epub 2018 Apr 6 PMID: 29574749.

Paaventhan, P., Joseph, J. S., Seow, S. V., Vaday, S., Robinson, H., Chua, K. Y., & Kolatkar, P. R. (2003). A 1.7Å structure of Fve, a member of the new fungal immunomodulatory protein family. *Journal of Molecular Biology, 332*(2), 461–470. https://doi.org/10.1016/s0022-2836(03)00923-9. PMID: 12948495.

Huang, L., Sun, F., Liang, C., He, Y. X., Bao, R., Liu, L., & Zhou, C. Z. (2009). Crystal structure of LZ-8 from the medicinal fungus *Ganoderma lucidium. Proteins., 75*(2), 524–527. https://doi.org/10.1002/prot.22346. PMID: 19137616.

Cong, W. R., Xu, H., Liu, Y., Li, Q. Z., Li, W., & Zhou, X. W. (2014). Production and functional characterization of a novel fungal immunomodulatory protein FIP-SN15 shuffled from two genes of *Ganoderma* species. *ApplMicrobiolBiotechnol., 98*(13), 5967–5975. https://doi.org/10.1007/s00253-014-5539-4. Epub 2014 Feb 28 PMID: 24682474.

Liao, C. H., Hsiao, Y. M., Lin, C. H., Yeh, C. S., Wang, J. C., Ni, C. H., … Ko, J. L. (2008). Induction of premature senescence in human lung cancer by fungal immunomodulatory protein from *Ganoderma tsugae. Food ChemToxicol., 46*(5), 1851–1859. https://doi.org/10.1016/j.fct.2008.01.044. Epub 2008 Feb 2 PMID: 18329152.

Hsin, I. L., Ou, C. C., Wu, T. C., Jan, M. S., Wu, M. F., Chiu, L. Y., … Ko, J. L. (2011). GMI, an immunomodulatory protein from *Ganoderma microsporum*, induces autophagy in non-small cell lung cancer cells. *Autophagy., 7*(8), 873–882. https://doi.org/10.4161/auto.7.8.15698. Epub 2011 Aug 1 PMID: 21490426.

Liao, C. H., Hsiao, Y. M., Hsu, C. P., Lin, M. Y., Wang, J. C., Huang, Y. L., & Ko, J. L. (2006). Transcriptionally mediated inhibition of telomerase of fungal immunomodulatory protein from *Ganoderma tsugae* in A549 human lung adenocarcinoma cell line. *MolCarcinog., 45*(4), 220–229. https://doi.org/10.1002/mc.20161. PMID: 16402390.

Liao, C. H., Hsiao, Y. M., Sheu, G. T., Chang, J. T., Wang, P. H., Wu, M. F., … Ko, J. L. (2007). Nuclear translocation of telomerase reverse transcriptase and calcium signaling in repression of telomerase activity in human lung cancer cells by fungal immunomodulatory protein from *Ganoderma tsugae. BiochemPharmacol., 74*(10), 1541–1554. https://doi.org/10.1016/j.bcp.2007.07.025. Epub 2007 Jul 22 PMID: 17720143.

Chang, Y. C., Hsiao, Y. M., Wu, M. F., Ou, C. C., Lin, Y. W., Lue, K. H., & Ko, J. L. (2013). Interruption of lung cancer cell migration and proliferation by fungal immunomodulatory protein FIP-fve from *Flammulina velutipes. Journal of Agriculture and Food Chemistry, 61*(49), 12044–12052. https://doi.org/10.1021/jf4030272. Epub 2013 Nov 22 PMID: 24274472.

Xie, Y., Li, S., Sun, L., Liu, S., Wang, F., Wen, B., … Xin, F. (2018). Fungal Immunomodulatory Protein from *Nectria haematococca* Suppresses Growth of Human Lung Adenocarcinoma by Inhibiting the PI3K/Akt Pathway. *International Journal of Molecular Sciences, 19*(11), 3429. https://doi.org/10.3390/ijms19113429. PMID: 30388826; PMCID: PMC6274709

Wang, J. J., Wang, Y., Hou, L., Xin, F., Fan, B., Lu, C., … Li, S. (2019). Immunomodulatory Protein from *Nectria haematococca* Induces Apoptosis in Lung Cancer Cells via the P53 Pathway. *International Journal of Molecular Sciences, 20*(21), 5348. https://doi.org/10.3390/ijms20215348. PMID: 31661772; PMCID: PMC6862031

Troiani, T., Napolitano, S., Della Corte, C. M., Martini, G., Martinelli, E., Morgillo, F., & Ciardiello, F. (2016). Therapeutic value of EGFR inhibition in CRC and NSCLC: 15 years of clinical evidence. *ESMO Open., 1*(5), Article e000088. https://doi.org/10.1136/esmoopen-2016-000088. PMID: 27843640; PMCID: PMC5070253

Ta, N. L., Chakrabandhu, K., Huault, S., & Hueber, A. O. (2018). The tyrosine phosphorylated pro-survival form of Fas intensifies the EGF-induced signal in colorectal cancer cells through the nuclear EGFR/STAT3-mediated pathway. *Scientific Reports, 8*(1), 12424. https://doi.org/10.1038/s41598-018-30804-z. PMID: 30127519; PMCID: PMC6102278